ORGANOMETALLICS

Volume 5, Number 5, May 1986

Cycloheptatrienyl-Bridged Heterobimetallic Complexes: Facile Phosphine Substitution Reactions of $(\mu\text{-}C_7H_7)\overline{Fe(CO)_3}Rh(CO)_2$

Richard G. Ball,† Frank Edelmann, Gong-Yu Kiel,‡ and Josef Takats*

Department of Chemistry, University of Alberta, Edmonton, Alberta, Canada T6G 2G2

Ronald Drews†

Institut für Anorganische und Angewandte Chemie, Universität Hamburg, Martin-Luther-King Platz 6, 2000 Hamburg 13, West Germany

Received August 7, 1985

$(\mu\text{-}C_7H_7)\overline{Fe(CO)_3}Rh(CO)_2$ (**1a**) is conveniently prepared by the atmospheric pressure carbonylation of $(\mu\text{-}C_7H_7)\overline{Fe(CO)_3}Rh(COD)$ (**1b**). The solid-state structure of **1b** has been determined. It mirrors that of **1a** except for some 0.1-Å increase in the Fe–Rh bond length which is traced to electronic changes at Rh due to CO groups exchange for COD moiety. **1a** reacts readily with a variety of phosphine ligands to give mono- (**2**) and disubstituted (**3**) derivatives depending on the reaction stoichiometry. The substitution occurs exclusively at the Rh center. Contrary to **1a** which contains only terminal carbonyl groups, compounds **2** exist in solution as a mixture of all-terminal and carbonyl-bridged isomers, whereas compounds **3** exhibit only the latter isomeric form $(\mu\text{-}C_7H_7)(\mu\text{-}CO)\overline{Fe(CO)_2}Rh(PR_3)_2$. The presence of a bridging carbonyl group implies a reversal of the bonding mode of the $\mu\text{-}C_7H_7$ moiety from η^3-Fe, η^4-Rh in **1a** to η^4-Fe, η^3-Rh in **3**. This has been verified by X-ray structural analysis of one member, $2PR_3 = Ph_2PCH_2CH_2PPh_2$, **3b**. Variable-temperature ^{13}C NMR studies show that molecules **3** undergo localized bridge–terminal carbonyl group scrambling on the iron center, and the same process also occurs in **2** at low temperatures; however, at high temperatures global carbonyl scrambling between Fe and Rh is also observed. It is suggested that the variable-bonding capability of the $\mu\text{-}C_7H_7$ moiety is responsible for the facile carbonyl substitution in **1a** and carbonyl scrambling in compounds **2** and **3**.

Introduction

The synthesis and reactivity of heterobimetallic and cluster transition-metal complexes continues to attract considerable interest.[1] The main reason for this interest stems from the belief that by bringing together the diverse chemical characteristics of different metals in the same molecules, the complexes will present unique reactivity patterns not exhibited by the constituent monomeric fragments. However, to be useful as a catalyst or a catalyst precursor a compound must possess the ability to readily achieve coordinative unsaturation, yet the majority of the so far reported heterometallic complexes contain coordinately saturated metal centers.

Some time ago[2] we have reported the synthesis of $(\mu\text{-}C_7H_7)\overline{Fe(CO)_3}Rh(CO)_2$ (**1a**) and commented on its facile, nondiscriminate and high level of ^{13}CO enrichment which occurred at room temperature and under atmospheric conditions. In view of the known variable coordination mode of the cycloheptatrienyl moiety[3] a plausible scenario

Scheme I

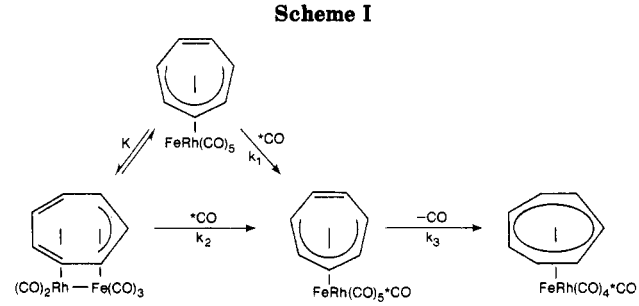

† X-ray structure.
‡ Nee Lin.

(1) (a) Roberts, D. A.; Geoffroy, G. L. "Comprehensive Organometallic Chemistry"; Wilkinson, G., Stone, F. G. A., Abel, E. W., Eds.; Pergamon Press: Oxford, 1982; Chapter 40. (b) "Reactivity of Metal-Metal Bonds"; Chisholm, M. H., Ed.; American Chemical Society: Washington, D.C., 1981; *ACS Symp. Ser. No. 155.*

(2) Bennett, M. J.; Pratt, J. L.; Simpson, K. A.; LiShingMan, L. K. K.; Takats, J. *J. Am. Chem. Soc.* **1976**, *98*, 4810.

0276-7333/86/2305-0829$01.50/0

for the rapid carbonyl exchange reaction in **1a** is presented in Scheme I. In the mechanism we postulate the ready accessibility of an intermediate with increased carbonyl content and having a bridging cycloheptatrienyl unit of reduced μ-η^5 hapticity. The intermediate then loses carbon monoxide thus completing the labeling sequence. As shown in Scheme I the intermediate could arise either by rapid equilibrium between μ-η^7 and μ-η^5 ring species of the starting material followed by *CO attack of the coordinately unsaturated μ-η^5 species or by a one step associative *CO addition. In either case the facility of the carbonyl exchange process must be associated with the ability of the μ-C_7H_7 moiety to provide coordinative unsaturation on the Fe–Rh framework. Such "incipient coordinative unsaturation" is not restricted to the present complex, and it has been used in order to explain the remarkable increase in the rate of carbonyl substitution of η^5-indenyl and η^5-fluorenyl compounds compared to the corresponding η^5-cyclopentadienyl derivatives.[4] It is worth noting at this juncture that the mechanism of the substitution reactions in the indenyl and fluorenyl complexes was established by careful kinetic measurements and is akin to the one presented in Scheme I.

As a first step in the reactivity studies with **1a** and as a means of pinpointing the site of the initial nucleophilic attack, we decided to investigate the phosphine substitution reaction of **1a**. The results of this study are reported here which also revealed an unexpected bonding mode change of the μ-C_7H_7 moiety on the Fe–Rh framework following phosphine substitution. In addition a much improved synthesis of **1a** is given which makes this interesting and reactive heterobimetallic complex available in a straightforward fashion and in good yield.[5]

Experimental Section

All experimental procedures were performed in standard Schlenk vessels under a static atmosphere of rigorously purified nitrogen or argon.[2] Solvents were dried by refluxing under nitrogen with the appropriate drying agent and distilled just prior to use. Trimethylphosphine, bis(diphenylphosphino)ethane (DPPE), bis(diphenylphosphino)methane (DPPM), and bis(dimethylphosphino)ethane (DMPE) were purchased from Strem Chemicals and triphenylphosphine, trimethyl phosphite, and 1,5-cyclooctadiene (COD) from Aldrich. Hydrated rhodium trichloride was obtained from Johnson Matthey, Inc. Methyldiphenylphosphine,[6] $[RhCl(COD)]_2$,[7] and $Na(C_7H_7)Fe(CO)_3$[8] were prepared by standard literature methods. The improved synthesis of $(\mu\text{-}C_7H_7)\overline{Fe(CO)_3Rh(CO)_2}$[2] is described below.

Infrared spectra were obtained with a Nicolet MX-1 Fourier transform interferometer. NMR spectra were recorded on a Bruker WP-200 or Bruker WP-400 spectrometer; for variable-temperature NMR studies sealed sample tubes were used. Mass spectra were taken with an A.E.I. MS-12 spectrometer operating at 70 or 16 eV. The samples were introduced into the ion source by using the direct inlet technique at a temperature just sufficient to record the data. Melting points are uncorrected and were determined on a Thomas-Hoover apparatus on samples which were sealed in a capillary. Elemental analyses were performed by the Microanalytical Laboratory of this department.

Preparation of the Complexes. Improved Synthesis of $(\mu\text{-}C_7H_7)\overline{Fe(CO)_3Rh(CO)_2}$ (1a). This compound was obtained in virtually quantitative yield by the room temperature and atmospheric pressure carbonylation of isolated or in situ prepared $(\mu\text{-}C_7H_7)\overline{Fe(CO)_3Rh(COD)}$.

$(\mu\text{-}C_7H_7)\overline{Fe(CO)_3Rh(COD)}$ (1b). A solution of 3.75 g (14.76 mmol) of $Na(C_7H_7)Fe(CO)_3$ in 50 mL of THF was added at room temperature over a period of 1 h to a solution of 3.60 g (7.30 mmol) of $[RhCl(COD)]_2$ in 150 mL of THF. The deep red-brown reaction mixture was stirred for an additional 1 h and then evaporated to dryness. The residue was extracted with 5 × 50 mL of boiling hexane, and the hexane solutions were filtered while hot. Concentrations of the combined extracts to 25 mL and cooling at −20 °C overnight gave 4.20 g (65% yield) of red crystals, mp 132 °C. An analytical sample was obtained by recrystallization from hexane.

Anal. Calcd for $C_{18}H_{19}FeO_3Rh$: C, 48.90; H, 4.33. Found: C, 49.14; H, 4.42. Mass spectrum (70 eV, 80 °C): *m/e* (relative intensity) 442 (M^+, 19.4), 414 ($M^+ - CO$, 32.7), 386 ($M^+ - 2CO$, 11.4), 358 ($M^+ - 3CO$, 100). IR (hexane): ν_{CO} 2007, 1943 cm^{-1}. ^1H NMR (25 °C, CD_2Cl_2, 200 MHz): δ 3.76 (s br, CH_{COD}, 4 H), 3.74 (s, C_7H_7, 7 H), 2.44 (m, $CH_{2,COD}$, 4 H), 2.24 (m, $CH_{2,COD}$, 4 H). ^{13}C NMR (25 °C, CD_2Cl_2, 50.32 MHz): δ 217.6 (s, CO_{Fe}), 84.2 (d, CH_{COD}, J_{Rh-C} = 9.6 Hz), 65.0 (s, C_7H_7), 31.8 (s, $CH_{2,COD}$).

$(\mu\text{-}C_7H_7)\overline{Fe(CO)_3Rh(CO)_2}$ (1a). A solution of 1.37 g (5.39 mmol) of $Na(C_7H_7)Fe(CO)_3$ in 25 mL of THF was added at room temperature over 1 h to 1.32 g (2.68 mmol) of $[RhCl(COD)]_2$ suspended in 25 mL of THF. The reddish brown reaction mixture was stirred for 1 h and evaporated to dryness. The residue was dissolved in 30 mL of warm toluene and chromatographed on a 10-cm silica gel column (Merck, Kieselgel 60 mesh). Elution with toluene produced a large red band. The solvent was removed from the eluate, and the residue was redissolved in 150 mL of hexane. A rapid stream of CO was bubbled through the solution for 5 min. At this stage the IR spectrum of the solution indicated a complete conversion to **1a**. Removal of the solvent in vacuo followed by washing the residue with 10 mL of cold (~−100 °C) pentane gave 1.35 g (65% yield) of pure **1a** as red-brown crystals.

Synthesis of Phosphine-Substituted Derivatives of 1. Since all the compounds were obtained by the same general procedure only a synopsis of the method is given followed by the amounts of material used and some physical characteristics of individual complexes.

Stoichiometric amounts of the appropriate phosphines were added to a solution of **1a** in hexane. The reaction mixtures were stirred at room temperature for 30 min to 2 h during which time the products, with the exception of $(\mu\text{-}C_7H_7)FeRh(CO)_4(PMe_3)$ (**2a**) which had to be cooled in dry ice, precipitated. Filtration followed by washing with hexane or pentane and drying in vacuo gave, except when indicated otherwise, analytically pure solid products.

$(\mu\text{-}C_7H_7)FeRh(CO)_4(PMe_3)$ (2a). **1a** (0.0807 g, 0.207 mmol) and PMe_3 (0.021 mL, 0.0157 g, 0.207 mmol) in 20 mL of hexane gave 0.082 g (91% yield) of red solid, mp 109–111 °C dec.

Anal. Calcd for $C_{14}H_{16}FeO_4PRh$: C, 38.39; H, 3.68. Found: C, 38.05; H, 3.78. Mass spectrum (16 eV, 70 °C): M^+, $M^+ - nCO$ (n = 1–4).

$(\mu\text{-}C_7H_7)FeRh(CO)_4(PPh_3)$ (2b). **1a** (0.300 g, 0.769 mmol) and PPh_3 (0.200 g, 0.763 mmol) in 75 mL of hexane gave 0.331 g (69% yield) or red crystalline solid, mp 143–145 °C dec.

Anal. Calcd for $C_{29}H_{22}FeO_4PRh$: C, 55.80; H, 3.55. Found: C, 55.77; H, 3.68. Mass spectrum (70 eV, 125 °C): M^+, $M^+ - nCO$ (n = 1–4).

$(\mu\text{-}C_7H_7)FeRh(CO)_3(PMe_3)_2$ (3a). **1a** (0.085 g, 0.218 mmol) and PMe_3 (0.0443 mL, 0.0331 g, 0.436 mmol) in 30 mL of hexane gave 0.0635 g (60% yield) of brown solid, mp 121–125 °C dec.

Anal. Calcd for $C_{16}H_{25}FeO_3P_2Rh$: C, 39.54; H, 5.18. Found: C, 35.36; H, 4.81. Mass spectrum (16 eV, 165 °C): M^+, $M^+ - nCO$ (n = 1–3), $M^+ - 3CO - PMe_3$.

$(\mu\text{-}C_7H_7)FeRh(CO)_3(DPPE)$ (3b). **1a** (0.053 g, 0.136 mmol) and DPPE (0.0541 g, 0.136 mmol) in 20 mL of hexane gave 0.090

(3) Examples of η^1 (Heinekey, D. M.; Graham, W. A. G. *J. Am. Chem. Soc.* **1979**, *101*, 6115), η^3 (Sepp, E.; Pürzer, A.; Thiele, G.; Behrens, H. *Z. Naturforsch., B: Anorg. Chem., Org. Chem.* **1978**, *33B*, 261), η^5 (Whitesides, T. H.; Budnik, R. A. *Inorg. Chem.* **1976**, *15*, 874), η^7 (Green, M. L. H.; Pardy, R. B. A. *Polyhedron* **1985**, *4*, 1035) bonding arrangements have been reported.

(4) (a) Rerek, M. E.; Ji, L.-N.; Basolo, F. *J. Chem. Soc., Chem. Commun.* **1983**, 1208. (b) Ji, L.-N.; Rerek, M. E.; Basolo, F. *Organometallics* **1984**, *3*, 740. (c) Rerek, M. E.; Basolo, F. *J. Am. Chem. Soc.* **1984**, *106*, 5908.

(5) Preliminary report on portions of this work: Lin, G.-Y.; Takats, J. *J. Organomet. Chem.* **1984**, *269*, C4.

(6) Markham, R. T.; Dietz, E. A., Jr.; Martin, D. R. *Inorg. Synth.* **1976**, *16*, 157.

(7) Giordano, G.; Crabtree, R. H. *Inorg. Synth.* **1979**, *19*, 218.

(8) Moll, M.; Behrens, H.; Kellner, R.; Knöchel, H.; Würstl, P. *Z. Naturforsch., B: Anorg. Chem., Org. Chem.* **1976**, *31B*, 1019.

Table I. Crystallographic Data

	$(\eta\text{-}C_7H_7)\overline{Fe(CO)_3Rh}(COD)$	$(\mu\text{-}C_7H_7)FeRh(CO)_3(DPPE)$
formula	$C_{18}H_{19}FeO_3Rh$	$C_{36}H_{31}FeO_3P_2Rh$
fw	442.10	732.35
space group	$P2_1/1c$	$I2/a$
a, Å	10.274 (4)	22.496 (4)
b, Å	13.504 (5)	10.695 (3)
c, Å	11.911 (3)	27.362 (2)
β, deg	98.18 (2)	111.17 (1)
V, Å^3	1635.7	6138.75
Z	4	8
d_{calcd}, g/cm^3	1.80	1.58
cryst size, mm	0.15 × 0.15 × 0.30	
diffractometer	Syntex $P2_1$	Enraf-Nonius CAD-4F
temp, °C	22	22
radiatn (incident beam monochromated)	Mo Kα	Mo Kα
scan mode	θ–2θ	ω–2θ
2θ limits, deg	2–58	2–50
no. of unique data ($F_o > 3\sigma(F_o)$)	2824	2206
abs. correction	none	none
linear abs coeff μ, cm^{-1}	17.70	11.37
no. of parameters refined	284	234
R	0.056	0.057
R_w	0.056	0.066

g of crude **3b**. Recrystallization from benzene/hexane afforded **3b** in ~50% yield as black needles, mp 226 °C dec.

Anal. Calcd for $C_{36}H_{31}FeO_3P_2Rh$: C, 59.04; H, 4.27; O, 6.55. Found: C, 59.79; H, 4.27; O, 6.88. Mass spectrum (16 eV, 185 °C): M^+, $M^+ - n$CO (n = 1–3).

The same material can be obtained directly from $(\mu\text{-}C_7H_7)Fe(CO)_3Rh(COD)$. To 0.330 g (0.75 mmol) of **1b** in 50 mL of toluene was added a solution of 0.300 g (0.75 mmol) of DPPE in 100 mL of toluene, and the mixture was stirred at 90 °C for 2 h. The color of the solution changed from red to black. The reaction mixture was evaporated to dryness, and the residue was washed with 2 × 50 mL of boiling hexane. After drying in vacuo, 0.320 g (59% yield) of gray-black microcrystalline solid **3b** was obtained.

$(\mu\text{-}C_7H_7)FeRh(CO)_3$(DPPM) (3c). **1a** (0.092 g, 0.236 mmol) and DPPM (0.0906 g, 0.236 mmol) in 50 mL of hexane gave 0.163 g (96% yield) of black solid, mp 193–195 °C dec.

Anal. Calcd for $C_{35}H_{29}FeO_3P_2Rh$: C, 58.52; H, 4.07. Found: C, 58.24; H, 4.10. Mass spectrum (16 eV, 170 °C): $M^+ - 2$CO, $M^+ - 3$CO.

$(\mu\text{-}C_7H_7)FeRh(CO)_3$(DMPE) (3d). **1a** (0.059 g, 0.151 mmol) and DMPE (0.025 mL, 0.0225 g, 0.150 mmol) in 20 mL of hexane gave 0.066 g (90% yield) of red-brown solid, mp 173–178 °C dec.

Anal. Calcd for $C_{16}H_{23}FeO_3P_2Rh$: C, 39.70; H, 4.79. Found: C, 36.64; H, 4.83. Mass spectrum (16 eV, 140 °C): M^+, $M^+ - n$CO (n = 1–3).

$(\mu\text{-}C_7H_7)FeRh(CO)_3[P(OMe)_3]_2$ (3e). **1b** (0.221 g, 0.50 mmol) and $P(OMe)_3$ (0.20 mL, 1.53 mmol) in 20 mL of hexane gave 0.278 g (96% yield) of black-violet crystals, mp 122 °C.

Anal. Calcd for $C_{16}H_{25}FeO_9P_2Rh$: C, 33.02, H, 4.33. Found: C, 32.83; H, 4.32. Mass spectrum (16 eV, 110 °C): M^+, $M^+ - n$CO (n = 1–3).

$(\mu\text{-}C_7H_7)FeRh(CO)_3(PMePh_2)_2$ (3f). To a solution of **1b** (0.221 g, 0.50 mmol) in 25 mL of hexane was added 0.30 g (1.50 mmol) of $PMePh_2$. The solution turned violet, and black crystals began to precipitate. The suspension was stirred for 30 min at room temperature. The precipitate was filtered off, washed with 2 × 10 mL of pentane, and dried in vacuo to give 0.300 g (82% yield) of glistening black crystals, mp 192 °C.

Anal. Calcd for $C_{36}H_{33}FeO_3P_2Rh$: C, 58.88; H, 4.53. Found: C, 58.45, H, 4.60. Mass spectrum (16 eV, 170 °C): $M^+ - 3$CO.

Synthesis of ^{13}CO-Enriched Samples. ^{13}CO (90%) was purchased from Monsanto Research Corp. Compounds **2** were enriched in ^{13}CO by stirring a benzene solution of the materials under 1 atm of ^{13}CO for 4 h, repeating the procedure under a fresh atmosphere of ^{13}CO resulted in >80% enrichment. ^{13}C-enriched compounds **3** were obtained by treating previously ^{13}CO-labeled **1a** with the appropriate phosphines in hexane.

X-ray Structure Determinations. A summary of the important technical details is given in Table I. Intensity measurements on $(\mu\text{-}C_7H_7)\overline{Fe(CO)_3Rh}(COD)$ were performed as described previously.[9] The structure was solved by using the direct method[10] and refined, all hydrogen atoms isotropic and all other atoms anisotropic, by using full-matrix least-squares techniques. The data collection routine for $(\mu\text{-}C_7H_7)FeRh(CO)_3(DPPE)$ has been described also.[11] Solution and refinement of the structures were accomplished by Patterson synthesis and the usual combination of least-squares refinements and Fourier synthesis.[12] The carbon atoms of the cycloheptatrienyl moiety and those of the phenyl rings were refined isotropically, the remaining non-hydrogen atoms were treated anisotropically, and hydrogen atoms were not included in the refinement. Atomic scattering factors and anomalous dispersion terms were taken from the usual sources.[13]

Results and Discussion

Improved Synthesis of $(\mu\text{-}C_7H_7)\overline{Fe(CO)_3Rh}(CO)_2$ (1a). Originally complex **1** was obtained in only 15% isolated yield from the reaction of $LiFe(C_7H_7)(CO)_3$ with $[Rh(CO)_2Cl]_2$ (eq 1).[2] The reaction was accompanied by

$$LiFe(C_7H_7)(CO)_3 + {}^1/_2[Rh(CO)_2Cl]_2 \xrightarrow[-20\ °C]{THF} \underset{\mathbf{1a}}{(\mu\text{-}C_7H_7)\overline{Fe(CO)_3Rh}(CO)_2} + [Fe(\eta^4\text{-}C_7H_7)(CO)_3]_2 + [Rh(CO)_x]_y + \ldots \quad (1)$$

the formation of large amounts of undesirable side products which rendered isolation of **1a** tedious. This coupled with the low synthetic yield hampered the initiation of a full scale reactivity study on **1a**.[14] To eliminate the production of reduced rhodium carbonyl species and hence quench the electron-transfer reductive pathway open to $Fe(C_7H_7)(CO)_3^-$, we were led to investigate the reaction of this anion with $[Rh(COD)Cl]_2$. The reaction proceeded

(9) Wormsbächer, D.; Edelmann, F.; Behrens, U. *Chem. Ber.* **1981**, *114*, 153.

(10) Sheldrick, G. SHELX, Programs for Crystal Structure Determination, Cambridge 1975.

(11) LiShingMan, L. K. K.; Reuvers, J. G. A.; Takats, J.; Deganello, G. *Organometallics* **1983**, *2*, 28.

(12) The computer programs used in this analysis include the Enraf-Nonius Structure Determination Package by B.A. Frenz ("Computing in Crystallography"; Delft University Press: Delft, Holland, 1978, pp 64–71) and several locally written or modified programs.

(13) "International Tables for X-ray Crystallography"; Kynoch Press: Birmingham, England, 1974; Vol. IV. Tables 2.2B and 2.3.1.

(14) The use of the more effective $KFe(C_7H_7)(CO)_3$[11] in reaction 1 resulted only in marginal improvement of the yield to 20–25%: Kiel, G.-Y.; Takats, J., unpublished observations.

readily, and hot extraction of the crude reaction mixture with hexane followed by crystallization afforded (μ-C_7H_7)Fe(CO)$_3$Rh(COD) (**1b**) in 65% yield. Crucial to the synthesis of **1a** was the find that purging a hexane solution of the cyclooctadiene derivative with CO at room temperature resulted in a quantitative conversion to **1a**. Presently, combination of in situ prepared (μ-C_7H_7)Fe(CO)$_3$Rh(COD) followed by atmospheric carbonylation routinely gives **1a** in 65% isolated yield, a 3–4-fold increase over the previous synthesis. It should be noted that the lability of COD in (μ-C_7H_7)Fe(CO)$_3$Rh(COD) makes this compound in many instances a viable alternative to **1a** for reactivity studies.

Characterization and Molecular Structure of (μ-C_7H_7)Fe(CO)$_3$Rh(COD) (1b).[15] As described above the reaction between Fe(C_7H_7)(CO)$_3^-$ and [Rh(COD)Cl]$_2$ gives, after a simple workup, moderate yields of a red crystalline material which on the basis of elemental analysis and spectroscopic studies can be formulated as (μ-C_7H_7)Fe(CO)$_3$Rh(COD) (**1b**). The mass spectrum of **1b** shows a parent molecular ion followed by the successive loss of three carbonyl groups. The IR spectrum exhibits two strong absorptions in the terminal carbonyl region due to the Fe(CO)$_3$ moiety. The lower frequency absorption at 1943 cm^{-1} is some 15 cm^{-1} lower than the corresponding band in **1a** consistent with more electron density and hence stronger back-bonding from Fe to the carbonyl groups upon replacing the CO ligands on Rh with the weaker π-acidic COD ligand. The ^{1}H NMR spectrum at room temperature shows a sharp singlet for the C_7H_7 moiety, a broad singlet for the four olefinic hydrogens of the COD ligand, and two multiplets for the aliphatic CH_2 groups. Similarly in the ^{13}C NMR spectrum singlets are observed for the Fe(CO)$_3$ moiety, C_7H_7 ring, and the aliphatic carbons of the COD group; the olefinic carbons of the latter are seen as a sharp doublet (J_{Rh-C} = 9.6 Hz) which conclusively demonstrates that the COD ligand remained bonded to the Rh atom in **1b**. The observation of single lines in the NMR spectra indicates that both C_7H_7 and COD moieties are undergoing fluxional movement in the molecule as well as local carbonyl scrambling on Fe is occurring also. Although the limiting spectrum could not be reached, at −80 °C in the ^{1}H NMR spectrum one of the averaged CH_2 signals has clearly been split into two broad unresolved peaks separated by 80 Hz, indicating a slowing down of COD rotation about the Rh atom. The signal due to the other CH_2 groups has undergone some line-shape changes but remained a single peak. The behavior of the olefinic proton resonance is unfortunately unclear since it moves and remains under the C_7H_7 peak which only slightly broadens at low temperature, diagnostic of a still rapidly whizzing cycloheptatrienyl ring. From the coalescence temperature of the exchanging aliphatic hydrogens (−30 °C) the approximate value of the free energy of activation, $\Delta G^{\ddagger}_{T_c}$, for COD rotation is calculated to be 11.6 kcal/mol.[16]

The dynamic behavior observed in **1b** is not surprising, indeed it has become the norm for molecules containing similar molecular fragments. Thus in the parent carbonyl compound **1a**, the resonance due to μ-C_7H_7 only broadened at −164 °C and carbonyl scrambling was still occurring at this temperature also.[2] Similarly cyclooctadiene rotation in the isoelectronic cationic cyclooctatetraene complex (μ-C_8H_8)Fe(CO)$_3$Rh(COD)$^+$ has been established by Salzer.[17] Although the activation energy for COD rotation in the latter complex was not calculated, the observation of broad signals for the COD unit already at room temperature and limiting spectrum at −60 °C appear to indicate more hindered rotation of the cyclooctadiene ligand in the cationic compound than in the neutral **1b**. This is surprising in view of the apparent stronger Rh–diene bonding in **1b** as reflected by the larger coordination shift of the olefinic carbons of the COD ring ($\delta(CH_{COD})$ for (μ-C_7H_7)Fe(CO)$_3$Rh(COD) 84.2 and for (μ-C_8H_8)Fe(CO)$_3$Rh(COD)$^+$ 92.1).[18]

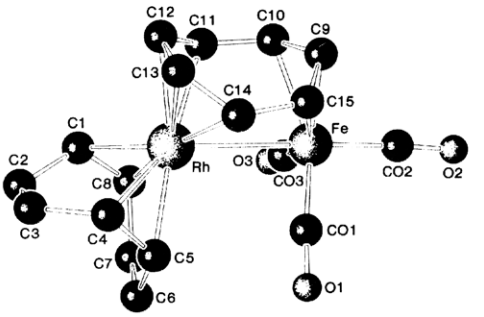

Figure 1. Perspective view of (μ-C_7H_7)Fe(CO)$_3$Rh(COD) (**1b**) showing the atom numbering scheme.

On the basis of the low-temperature ^{1}H NMR results which indicate two different types of aliphatic and hence olefinic carbons for the Rh-bound cyclooctadiene, two structural forms, A and B, can be drawn for **1b**. The two

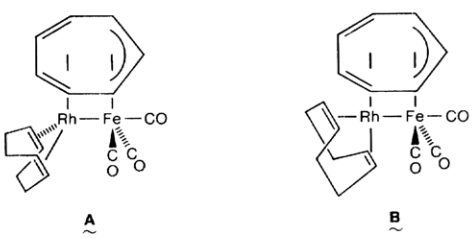

forms differ only in the orientation of the COD ring. In A the double bonds occupy equivalent coordination sites on the rhodium, trans to the bridging cycloheptatrienyl ring, akin to the positions of the carbonyl ligands on rhodium in **1a**.[2] On the other hand, in B, the COD ligand occupies two nonequivalent coordination sites, one double bond being trans to the Fe–Rh bond and the other trans to the C_7H_7 ring. It should be noted that the symmetry of both structures is C_s which requires two different olefinic and aliphatic COD carbons in the low-temperature limiting spectrum. Thus NMR alone is not sufficient to deduce the ground-state structure of **1b**.[19] In order to unequivocally establish its structure and to compare it to the analogous pentacarbonyl **1a**, a X-ray structure analysis on **1b** was carried out.

(15) (a) This compound has also been described by Salzer et al.[15b] In general our data are in good agreement with theirs, and only a few complementary points are discussed in the present contribution. (b) Salzer, A.; Egolf, T.; von Philipsborn, W. *Helv. Chim. Acta* **1982**, *65*, 1145.

(16) (a) Kost, D.; Carlson, E. H.; Raban, M. *J. Chem. Soc., Chem. Commun.* **1971**, 665. (b) Although the exchanging sites are not singlets, approximating them as such in order to apply the expression for $\Delta G^{\ddagger}_{Tc}$ does not seriously effect the value of the latter.

(17) Salzer, A.; Egolf, T.; von Philipsborn, W. *J. Organomet. Chem.* **1981**, *221*, 351.

(18) As expected, the $\Delta G^{\ddagger}_{Tc}$ for COD rotation in the Ir analogue of **1b** at 15.7 kcal/mol is a higher energy process: Edelmann, F.; Takats, J., manuscript in preparation.

(19) Both forms have been postulated for Rh-bound COD ligand in heterobimetallic Rh–Fe complexes.[15b,17]

Table II. Final Atomic Positional Parameters for (μ-C_7H_7)Fe(CO)$_3$Rh(COD) (1b)[a]

	x/a	y/b	z/c
Rh	0.2110 (1)	0.4224 (1)	0.2762 (1)
Fe	0.4215 (1)	0.3715 (1)	0.1534 (1)
CO(1)	0.3539 (9)	0.2513 (8)	0.1649 (8)
O(1)	0.3152 (8)	0.1709 (5)	0.1663 (7)
CO(2)	0.5569 (8)	0.3323 (8)	0.0897 (8)
O(2)	0.6417 (7)	0.3033 (6)	0.0432 (7)
CO(3)	0.3270 (8)	0.4117 (7)	0.0261 (8)
O(3)	0.2706 (7)	0.4387 (6)	-0.0596 (6)
C(1)	0.0250 (8)	0.4985 (7)	0.2214 (8)
C(2)	-0.0823 (11)	0.4659 (12)	0.2868 (11)
C(3)	-0.0446 (11)	0.3945 (10)	0.3790 (12)
C(4)	0.0820 (10)	0.3386 (8)	0.3695 (8)
C(5)	0.1039 (8)	0.2805 (7)	0.2783 (7)
C(6)	0.0038 (10)	0.2671 (8)	0.1738 (9)
C(7)	-0.0024 (11)	0.3489 (8)	0.0853 (10)
C(8)	0.0607 (7)	0.4449 (6)	0.1295 (7)
C(9)	0.5395 (9)	0.4570 (9)	0.2650 (9)
C(10)	0.4492 (9)	0.5253 (8)	0.2086 (8)
C(11)	0.3306 (9)	0.5537 (6)	0.2491 (8)
C(12)	0.3040 (10)	0.5516 (8)	0.3633 (9)
C(13)	0.3319 (9)	0.4707 (8)	0.4343 (8)
C(14)	0.3905 (9)	0.3851 (9)	0.3940 (8)
C(15)	0.4998 (9)	0.3796 (9)	0.3291 (8)
H(1)	0.0508 (68)	0.5689 (60)	0.2251 (59)
H(21)	-0.1274 (112)	0.5208 (87)	0.3068 (95)
H(22)	-0.1462 (104)	0.4333 (81)	0.2297 (92)
H(31)	-0.1220 (105)	0.3608 (79)	0.3912 (86)
H(32)	-0.0174 (116)	0.4268 (90)	0.4540 (100)
H(4)	0.1197 (92)	0.3242 (72)	0.4313 (80)
H(5)	0.1668 (83)	0.2300 (67)	0.3023 (71)
H(61)	-0.0796 (66)	0.2667 (49)	0.2005 (52)
H(62)	0.0239 (113)	0.2124 (90)	0.1362 (98)
H(71)	0.0460 (75)	0.3289 (58)	0.0362 (65)
H(72)	-0.0872 (132)	0.3611 (102)	0.0679 (110)
H(8)	0.0971 (76)	0.4817 (63)	0.0750 (71)
H(9)	0.6143 (78)	0.4639 (60)	0.2490 (65)
H(10)	0.4850 (96)	0.5713 (79)	0.1477 (83)
H(11)	0.2716 (84)	0.6031 (64)	0.2014 (73)
H(12)	0.2602 (65)	0.5946 (51)	0.3851 (58)
H(13)	0.3074 (88)	0.4701 (72)	0.5102 (83)
H(14)	0.3899 (58)	0.3330 (47)	0.4372 (52)
H(15)	0.5526 (78)	0.3316 (60)	0.3463 (69)

[a] Estimated standard deviations in this and other crystallographic tables are given in parentheses and correspond to the last significant digits.

A perspective view of the molecule together with the atomic numbering scheme is shown in Figure 1. Table II lists the final atomic positional parameters for **1b**, and selected bond distances and angles can be found in Table III. It is clear from the figure that the structural work corroborates the molecular formulation based on spectroscopic studies and furthermore shows that of the two structural forms compatible with the spectral results the ground-state structure of the molecule is of the form A. Very similar arrangement of ligands around the Fe–Rh framework was also shown by the related pentacarbonyl compound **1a**. The only difference being the replacement of two carbonyl ligands on Rh in **1a** by the double bonds of the COD moiety in **1b**. Evidently in both **1a** and **1b** the geometrical preference of Rh is for square-pyramidal geometry and not for the alternate trigonal-bipyramidal arrangement for five-coordination exhibited by form B. The related compound $Rh(C_4H_6)_2Cl$ (C_4H_6 = 1,3-butadiene) also contains a square-pyramidal rhodium atom.[20] The distances within the C_7H_7 ring and between the ring and the Fe–Rh framework are very similar to those found in **1a** and, as discussed fully before,[2] are typical for Rh–

(20) Immirze, A.; Allegra, G. *Acta Crystallogr., Sect. B: Struct. Crystallogr. Cryst. Chem.* **1969**, *25B*, 120.

Table III. Selected Interatomic Distances and Angles in (μ-C_7H_7)Fe(CO)$_3$Rh(COD) (1b)

Bond Lengths (Å)

Rh–Fe = 2.862 (1)

Rh–C(1)	2.186 (8)	Fe–C(9)	2.028 (9)
Rh–C(4)	2.165 (9)	Fe–C(10)	2.184 (10)
Rh–C(5)	2.210 (9)	Fe–C(15)	2.136 (9)
Rh–C(8)	2.182 (7)	Fe–CO(1)	1.779 (10)
Rh–C(11)	2.208 (8)	Fe–CO(2)	1.758 (11)
Rh–C(12)	2.181 (9)	Fe–CO(3)	1.766 (9)
Rh–C(13)	2.202 (9)	CO(1)–O(1)	1.157 (11)
Rh–C(14)	2.211 (9)	CO(2)–O(2)	1.164 (11)
		CO(3)–O(3)	1.158 (10)
C(1)–C(2)	1.503 (14)	C(9)–C(10)	1.409 (14)
C(2)–C(3)	1.471 (17)	C(10)–C(11)	1.425 (13)
C(3)–C(4)	1.522 (14)	C(11)–C(12)	1.426 (14)
C(4)–C(5)	1.385 (13)	C(12)–C(13)	1.387 (15)
C(5)–C(6)	1.509 (12)	C(13)–C(14)	1.418 (14)
C(6)–C(7)	1.522 (14)	C(14)–C(15)	1.452 (13)
C(7)–C(8)	1.510 (13)	C(15)–C(9)	1.389 (15)
C(8)–C(1)	1.404 (12)		

Bond Angles (deg)

C(2)–C(1)–C(8)	123.0 (10)	Rh–Fe–CO(1)	81.2 (3)
C(1)–C(2)–C(3)	116.4 (9)	Rh–Fe–CO(2)	174.1 (3)
C(2)–C(3)–C(4)	114.0 (9)	Rh–Fe–CO(3)	90.1 (3)
C(3)–C(4)–C(5)	125.1 (10)	Rh–Fe–C(9)	87.3 (3)
C(4)–C(5)–C(6)	123.2 (9)	Rh–Fe–C(10)	72.2 (3)
C(5)–C(6)–C(7)	116.1 (8)	Rh–Fe–C(15)	72.1 (3)
C(6)–C(7)–C(8)	114.1 (8)	Fe–Rh–C(1)	130.7 (3)
C(1)–C(8)–C(7)	124.6 (9)	Fe–Rh–C(4)	134.4 (3)
C(10)–C(9)–C(15)	122.0 (9)	Fe–Rh–C(5)	102.2 (2)
C(9)–C(10)–C(11)	123.5 (10)	Fe–Rh–C(8)	97.1 (2)
C(10)–C(11)–C(12)	127.4 (10)	Fe–Rh–C(11)	69.0 (2)
C(11)–C(12)–C(13)	123.1 (10)	Fe–Rh–C(12)	97.1 (3)
C(12)–C(13)–C(14)	119.8 (9)	Fe–Rh–C(13)	97.6 (3)
C(13)–C(14)–C(15)	128.2 (10)	Fe–Rh–C(14)	69.3 (3)
C(9)–C(15)–C(14)	124.3 (10)		
Fe–CO(1)–O(1)	175.0 (9)	CO(1)–Fe–CO(2)	95.7 (5)
Fe–CO(2)–O(2)	176.2 (9)	CO(1)–Fe–CO(2)	100.0 (4)
Fe–CO(3)–O(3)	176.7 (8)	CO(2)–Fe–CO(3)	95.4 (4)

diene and Fe–allyl interactions. Indeed it is perhaps surprising that the replacement of two strongly π-acidic carbonyl ligands on Rh by less electron-withdrawing COD moiety and the corresponding changes in the retrodative bonding between Rh and the diene portion of the ring have not resulted in more drastic changes in C–C bond lengths (the appropriate distances which are identical within experimental error: **1a**, 1.422 (7), 1.379 (7), and 1.434 (7) Å; **1b**, 1.418 (14), 1.387 (15), and 1.426 (14) Å). However this is not the first case when subtle bonding changes remain elusive to X-ray detection. The Rh–C bond lengths to COD and C_7H_7 moieties are plagued by the same uncertainties. Although individual distances are not significantly different, on the whole the marginally shorter bond lengths to the cycloheptatrienyl ring is what expected from the stronger bonding interaction with a conjugated 1,3-diene system as opposed to the virtually independent two Rh–olefin type interactions with the COD ligand. The one significant and large difference between the two structures occurs in the length of the Fe–Rh bond distance. This distance, already long in **1a** (2.764 (1) Å compared to an average of 2.59 Å for unsupported Fe–Rh bond length[1a]), is some 0.1 Å longer in **1b** (2.862 (1) Å). Surprisingly, a survey of the distances between the COD ligand and eclipsed carbonyl groups revealed no unusually short contacts (the shortest distances are O(1)–H(5) = 2.51 Å and O(3)–H(8) = 2.63 Å). Thus the lengthening of the Fe–Rh bond on going from **1a** to **1b** must be a consequence of the large electronic difference between the carbonyl and COD moieties. Reflecting the longer Fe–Rh bond is the slight increase in the angle between the normals to the planes

Table IV. IR and ^1H and ^{31}P NMR Data on $(C_7H_7)FeRh(CO)_4PR_3$ (2) and $(C_7H_7)FeRh(CO)_3(PR_3)_2$ (3) Complexes

PR_3	IR ν_{CO},[a] cm^{-1}		^1H NMR[b] $\delta_{C_7H_7}$	δ_{other} (J_{P-H}, Hz)		$^{31}P\{^1H\}$[c] NMR δ	J_{Rh-P}, Hz
$1PMe_3$, **2a**	2000 (s)	1790 (m)	3.45 (s)	Me	0.85 (d, 9.5)	−4.14 (d)	161.7
	1967 (s)						
	1912 (s)						
$1PPh_3$, **2b**	2000 (s)	1802 (m)	3.84 (s)	Ph	7.53–7.40 (m)	43.9 (d)	179.3
	1971 (s)						
	1930 (s)						
$2PMe_3$, **3a**	1948 (s)	1742 (m)	3.54 (s)	Me	0.81 (t)	−3.78 (d)	170.0
	1879 (s)						
DPPE, **3b**	1955 (s)	1759 (m)	3.80 (s)	Ph	7.71–7.24 (m)	67.43 (d)	178.2
	1891 (s)			CH_2	2.75 (br)		
					2.15 (br)		
DPPM, **3c**	1956 (s)	1758 (m)	4.04 (s)	Ph	7.36 (br)	−14.34 (d)	152.3
	1891 (s)			CH_2	4.30 (t, 10)		
DMPE, **3d**	1947 (s)	1738 (m)	3.79 (s)	CH_2	1.64 (m)	46.68 (d)	167.5
	1878 (s)			Me	1.34 (br)		
$2P(OMe)_3$, **3e**	1972 (s)	1773 (m)	3.92 (s)	Me	3.59 (t, 18)	152.95 (d)	279.4
	1906 (s)						
$2PMe(Ph)_2$, **3f**	1967 (s)	1747 (m)	3.44 (s)	Ph	7.5–7.1 (m)	27.30 (d)	186.3
	1902 (s)			Me	1.52 (m)		

[a] Solvent CH_2Cl_2. Abbreviations: s = strong, m = medium. [b] δ relative to Me_4Si, J in Hz, solvent CD_2Cl_2 except **3a** and **2a** where C_6D_6 was used. [c] δ relative to 85% H_3PO_4. Abbreviations for NMR data: s = singlet, d = doublet, t = triplet, m = multiplet, br = broad.

formed by the diene and allyl fragments from 56° in **1a** to 62° in **1b**, indicating more folded μ-C_7H_7 moiety in the latter complex.

Reaction of 1 with Phosphines. As expected from the facile ^{13}CO exchange reaction, **1a** reacts readily with a variety of phosphines to give mono- and disubstituted derivatives depending on the reaction stoichiometry (eq 2 and 3). The reactions proceed rapidly at room temperature in hydrocarbon solvent from which the respective phosphine-substituted derivatives, except **2a**, precipitate in virtually quantitative yields. Due to its greater solubility **2a** was obtained by low-temperature crystallization, whereas pure **3b** was obtained only after recrystallization of the original reaction product resulting in lower yields for this last derivative. The reactivity of **1b** was also briefly investigated, and it was found to react with 2 molar equiv of phosphine (eq 4). Interestingly **1b** did not react with triphenylphosphine, and even the reaction with DPPE required the use of toluene as solvent and application of slight heat to affect the substitution. The greater reluctance of **1b** toward phosphine substitution has been noted by Salzer,[15b] who observed reactions only with $P(OR)_3$ (R = Me, Ph) type ligands. Reaction of **1a** with excess PPh_3 resulted in monosubstitution only and formation of **3a**, giving evidence for some steric control of the substitution. When **1a** was reacted with 5 equiv of PMe_3, infrared evidence indicated the substitution for more than two CO groups; however, no pure compound could be isolated from the mixture of materials.

$$\mathbf{1a} + PR_3 \xrightarrow{\text{hexane}} (\mu\text{-}C_7H_7)FeRh(CO)_4PR_3 \quad (2)$$
$$\mathbf{2a},\ PR_3 = PMe_3$$
$$\mathbf{2b},\ PR_3 = PPh_3$$

$$\mathbf{1a} + 2PR_3 \xrightarrow{\text{hexane}} (\mu\text{-}C_7H_7)FeRh(CO)_3(PR_3)_2 \quad (3)$$
$$\mathbf{3a},\ 2PR_3 = 2PMe_3$$
$$\mathbf{3b},\ 2PR_3 = DPPE$$
$$\mathbf{3c},\ 2PR_3 = DPPM$$
$$\mathbf{3d},\ 2PR_3 = DMPE$$

$$\mathbf{1b} + 2PR_3 \rightarrow (\mu\text{-}C_7H_7)FeRh(CO)_3(PR_3)_2 \quad (4)$$
$$\mathbf{3b},\ 2PR_3 = DPPE$$
$$\mathbf{3e},\ 2PR_3 = 2P(OMe)_3$$
$$\mathbf{3f},\ 2PR_3 = 2PMePh_2$$

The ^{31}P NMR spectrum of both series of complexes (Table IV) showed only one doublet with characteristic ^{103}Rh–^{31}P coupling[21] establishing clearly and unambiguously that the phosphine ligands are bound to the rhodium atom. This is not surprising since Rh is known to form many stable 16e species[22] and therefore is more prone to accommodate the necessary coordinative unsaturation to initiate phosphine substitution (Scheme I). Interestingly even in the case of the DPPM ligand system, which favors the formation of ligand-bridged dimetal species,[23] the initial reaction product contains chelating DPPM moiety with both phosphorus atoms coordinated to rhodium.

Unexpectedly and contrary to the related pentacarbonyl derivatives **1a**, which contained terminal carbonyl groups only, the IR spectrum (Table IV) of complexes **2** and **3** indicated the presence of both terminal and bridging carbonyl moieties. In particular the simple three-band spectrum observed for compounds **3** is consistent with the formulation $(\mu\text{-}C_7H_7)(\mu\text{-}CO)\overline{Fe(CO)_2Rh(PR_3)_2}$ for the bis(phosphine) derivatives. The four-band spectrum for **2** in CH_2Cl_2 would also agree with such a structure. However, when the spectrum of **2b** was recorded in several different solvents, a more complicated behavior was indicated. Thus in THF, benzene, and CS_2 the highest frequency band had a pronounced shoulder, and especially in CS_2 the middle band was clearly resolved into two components (ν_{CO}/cm^{-1} in CS_2 for **2b**: 2010 (sh), 2002 (s), 1980 (s), 1970 (s), 1937 (s), 1817 (m)). The appearance of more than four ν_{CO} bands clearly shows that the monosubstituted derivatives **2** exist in solution as a mixture of isomers, the all-terminal form C and the carbonyl-bridged form D. As a final point

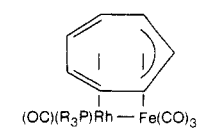

C

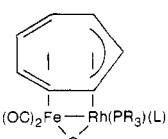

D

L = CO, 2; L = PR_3, 3

of interest the infrared spectrum of **2b** in Nujol mull shows

(21) Pregosin, P. S.; Kunz, R. H. "The ^{31}P and ^{13}C NMR of Transition Metal Phosphine Complexes"; Springer-Verlag: New York, 1979.
(22) Dixon, R. S. "Organometallic Chemistry of Rhodium and Iridium"; Academic Press: New York, 1983.
(23) Puddephatt, R. J. *Chem. Soc. Rev.* **1983**, *12*, 99.

Table V. Final Atomic Positional and Thermal Parameters for (μ-C_7H_7)(μ-CO)Fe(CO)$_2$Rh(DPPE) (3b)[a]

atom	x	y	z	U_{11}	U_{22}	U_{33}	U_{12}	U_{13}	U_{23}
Rh	73.74 (5)	128.82 (9)	402.22 (3)	32.1 (5)	26.4 (4)	28.4 (4)	1.5 (6)	8.5 (3)	2.3 (5)
Fe	50.01 (9)	332.8 (2)	454.32 (7)	48 (1)	32 (1)	39.6 (9)	0.0 (9)	16.3 (7)	-4.2 (8)
P(1)	147.6 (1)	136.1 (3)	363.6 (1)	31 (2)	35 (2)	37 (1)	1 (2)	9 (1)	1 (2)
P(2)	7.4 (2)	46.8 (3)	326.3 (1)	31 (2)	30 (2)	32 (2)	-1 (2)	8 (1)	-1 (1)
O(1)	44.0 (4)	374.0 (8)	345.7 (3)	60 (5)	41 (5)	43 (4)	10 (5)	16 (4)	9 (5)
O(2)	118.6 (5)	569 (1)	470.9 (4)	99 (8)	54 (6)	111 (8)	-21 (7)	14 (7)	-6 (7)
O(3)	-74.8 (4)	446 (1)	419.1 (4)	79 (6)	62 (7)	95 (6)	27 (6)	41 (5)	14 (6)
C(1)	51.1 (5)	313 (1)	384.3 (4)	41 (7)	28 (7)	37 (6)	-3 (6)	13 (5)	1 (6)
C(2)	93.3 (7)	472 (1)	464.7 (5)	61 (9)	49 (9)	56 (8)	-12 (8)	8 (7)	-9 (7)
C(3)	-24.9 (6)	405 (1)	431.5 (5)	54 (8)	36 (8)	60 (7)	16 (7)	26 (6)	4 (6)
C(4)	105.7 (5)	108 (1)	292.8 (4)	37 (6)	45 (8)	23 (5)	-1 (7)	8 (5)	0 (6)
C(5)	54.9 (5)	7 (1)	285.7 (4)	31 (7)	52 (8)	33 (6)	-12 (7)	10 (5)	-5 (6)
atom	z	y	z	U, Å^2	atom	x	y	z	U, Å^2
C(6)	32.0 (6)	240 (1)	514.0 (5)	53 (4)	C24	304.2 (6)	-169 (1)	418.1 (5)	53 (4)
C(7)	-0.4 (6)	165 (1)	469.1 (4)	45 (4)	C25	245.2 (6)	-185 (1)	425.5 (5)	48 (4)
C(8)	20.4 (6)	53 (1)	450.7 (4)	46 (4)	C26	199.2 (6)	-92 (1)	409.5 (4)	42 (4)
C(9)	83.6 (6)	3 (1)	467.8 (4)	46 (4)	C31	-30.8 (5)	-102 (1)	329.3 (4)	37 (3)
C(10)	136.9 (6)	88 (1)	484.7 (5)	55 (4)	C32	9.0 (6)	-209 (1)	348.8 (5)	48 (4)
C(11)	136.5 (6)	215 (1)	504.5 (5)	56 (4)	C33	-20.2 (6)	-324 (1)	351.5 (5)	52 (4)
C(12)	96.4 (6)	266 (1)	530.7 (5)	58 (4)	C34	-85.8 (6)	-330 (1)	339.3 (5)	52 (4)
C11	192.9 (5)	277 (1)	363.9 (4)	38 (3)	C35	-124.0 (6)	-226 (1)	322.1 (5)	53 (4)
C12	213.4 (6)	347 (1)	411.6 (5)	50 (4)	C36	-97.0 (5)	-110 (1)	317.0 (4)	43 (3)
C13	251.5 (7)	459 (1)	415.9 (5)	61 (4)	C41	-61.9 (5)	137 (1)	284.2 (4)	39 (3)
C14	264.4 (7)	489 (1)	371.6 (5)	68 (5)	C42	-91.0 (6)	216 (1)	308.4 (5)	52 (4)
C15	244.6 (6)	426 (1)	325.9 (5)	59 (4)	C43	-147.3 (7)	283 (1)	277.4 (5)	65 (5)
C16	206.5 (6)	317 (1)	320.4 (5)	54 (4)	C44	-170.8 (6)	265 (1)	224.5 (5)	63 (4)
C21	211.5 (5)	17 (1)	385.8 (4)	38 (3)	C45	-143.6 (7)	190 (1)	199.9 (5)	63 (4)
C22	269.5 (6)	33 (1)	377.7 (4)	44 (4)	C46	-86.8 (6)	120 (1)	229.3 (4)	48 (4)
C23	315.2 (6)	-63 (1)	394.3 (5)	57 (4)					

[a] All atomic parameters have been multiplied by 10^3. The form of the anisotropic thermal parameter is $\exp[-2\pi^2\{h^2a^{*2}U_{11} + k^2b^{*2}U_{22} + l^2c^{*2}U_{33} + 2hka^*b^*U_{12} + 2hla^*c^*U_{13} + 2klb^*c^*U_{23}\}]$.

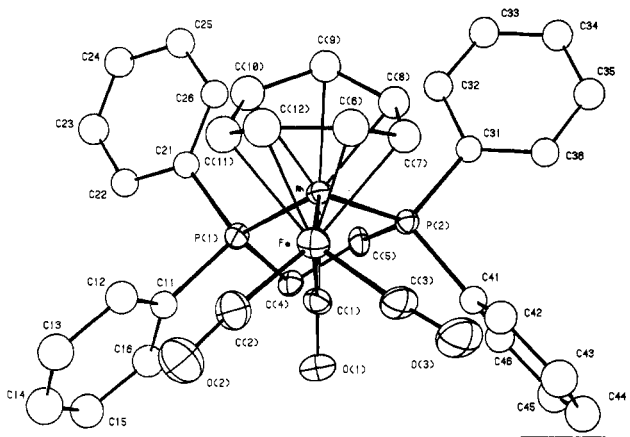

Figure 2. Perspective view of (μ-C_7H_7)(μ-CO)Fe(CO)$_2$Rh(DPPE) (**3b**) looking down the Fe–Rh bond and showing the complete atom numbering scheme.

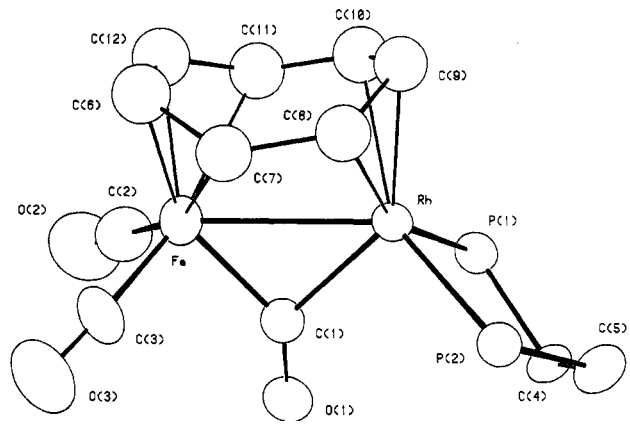

Figure 3. Perspective view of **3b** where the phenyl groups of the DPPE ligand have been removed for clarity.

only terminal carbonyl groups (ν_{CO}/cm^{-1}: 1997 (s), 1959 (s), 1921 (m), 1909 (m)) and indicates the presence of form C in the solid state. Simple electron counting reveals that formation of bridging carbonyl moiety must be accompanied by a reversal of the bonding mode between the Fe–Rh framework and the μ-C_7H_7 moiety upon phosphine substitution; this is clearly seen when form C and D are compared. To unequivocally verify this situation and to compare the structural features of **1a** and **1b** with that of a phosphine-substituted compound, the structure of **3b**, representative of the carbonyl-bridged isomer, was determined by X-ray crystallography.

Molecular Structure of (μ-C_7H_7)(μ-CO)Fe(CO)$_2$Rh(DPPE) (3b). Two perspective views of the molecule are shown in Figures 2 and 3. Figure 2 shows the complete atomic numbering scheme, whereas in Figure 3 the phenyl groups from the DPPE ligand have been omitted to give a clearer picture of the bonding arrangement in the molecule. Table V gives a listing of the final atomic and thermal parameters of **3b**, and selected bond distances and angles are listed in Table VI.

It is clear from the figures that the solid-state structure of **3b**, and by inference all other bis(phosphine) derivatives, conforms to bonding arrangement D. The basic (μ-C_7H_7)Fe–Rh framework is maintained, and the metal–metal bond is also bridged by a μ-CO ligand (Rh–C(1)–Fe angle is 87.6°). The bridge carbonyl bonding appears to be slightly asymmetric. The μ-CO ligand is 0.12 Å closer to the iron atom (Fe–C(1) = 1.93 (1) and Rh–C(1) = 2.05 (1) Å, respectively), and although most of this difference can be traced to changes in covalent metal radii, the slightly larger Fe–C(1)–O(1) angle (140.1 (8)°) compared to the Rh–C(1)–O(1) angle of 132.2 (8)° is also in accord with a stronger Fe–(μ-CO) interaction. A comparison of the bond distances of the FeRh(μ-CO) fragment with previous data is difficult since in the only other structurally characterized complex containing such unit [RhFeW(μ_3–

Table VI. Selected Interatomic Distances and Angles in (μ-C_7H_7)(μ-CO)$\overline{Fe(CO)_2}$Rh(DPPE) (3b)

Bond Lengths (Å)

Fe–Rh = 2.762 (2)

Rh–C(8)	2.25 (1)	C(6)–C(7)	1.42 (1)
Rh–C(9)	2.20 (1)	C(7)–C(8)	1.44 (1)
Rh–C(10)	2.24 (1)	C(8)–C(9)	1.44 (1)
Fe–C(7)	2.23 (1)	C(9)–C(10)	1.42 (1)
Fe–C(6)	2.07 (1)	C(10)–C(11)	1.47 (2)
Fe–C(12)	2.09 (1)	C(11)–C(12)	1.43 (2)
Fe–C(11)	2.30 (1)	C(12)–C(6)	1.39 (2)
Rh–C(1)	2.05 (1)	C(1)–O(1)	1.20 (1)
Fe–C(1)	1.93 (1)	C(2)–O(2)	1.16 (1)
Fe–C(2)	1.74 (1)	C(3)–O(3)	1.14 (1)
Fe–C(3)	1.75 (1)	P(1)–C(4)	1.85 (1)
Rh–P(1)	2.270 (3)	P(2)–C(5)	1.85 (1)
Rh–P(2)	2.252 (3)	C(4)–C(5)	1.53 (1)

Bond Angles (deg)

C(6)–C(7)–C(8)	130.0 (10)	Rh–Fe–C(7)	70.5 (3)
C(7)–C(8)–C(9)	126.7 (9)	Rh–Fe–C(6)	99.1 (3)
C(8)–C(9)–C(10)	119.0 (10)	Rh–Fe–C(12)	97.0 (3)
C(9)–C(10)–C(11)	125.9 (9)	Rh–Fe–C(11)	66.3 (3)
C(10)–C(11)–C(12)	128.5 (8)	Fe–Rh–C(8)	74.5 (3)
C(11)–C(12)–C(6)	122.0 (9)	Fe–Rh–C(9)	92.3 (3)
C(12)–C(6)–C(7)	123.0 (10)	Fe–Rh–C(10)	78.7 (3)
Fe–C(1)–Rh	87.6 (4)	Fe–Rh–C(1)	44.4 (3)
Rh–Fe–C(1)	47.9 (3)	Rh–C(1)–O(1)	132.2 (8)
Fe–C(1)–O(1)	140.1 (8)	Fe–Rh–P(1)	121.60 (8)
Rh–Fe–C(2)	124.2 (4)	Fe–Rh–P(2)	126.69 (8)
Rh–Fe–C(3)	120.4 (4)	P(1)–Rh–C(1)	91.0 (3)
Fe–C(2)–O(2)	175.0 (10)	P(2)–Rh–C(1)	97.5 (3)
Fe–C(3)–O(3)	175.0 (10)	P(1)–Rh–P(2)	86.3 (1)
C(2)–Fe–C(3)	95.2 (5)	Rh–P(1)–C(4)	107.4 (3)
C(2)–Fe–C(1)	93.3 (5)	P(1)–C(4)–C(5)	108.9 (6)
C(3)–Fe–C(1)	92.9 (5)	P(2)–C(5)–C(4)	109.2 (6)
		Rh–P(2)–C(5)	108.2 (3)

CC_6H_4Me-4)(μ-CO)$(CO)_5(\eta$-$C_5H_5)(\eta$-$C_9H_7)$],[24] the μ-CO unit bridging the Fe–Rh bond is definitely asymmetric, the carbonyl ligand being 0.09 Å closer to the rhodium atom (Rh–(μ-CO) = 1.928 (7) Å and Fe–(μ-CO) = 2.022 (7) Å). However, the Fe–(μ-CO) distance compares well with those found in homometallic complexes (cf. [Fe(η-C_5H_5)(μ-CO)$(CO)]_2$,[25] where the average Fe–(μ-CO) bond length is 1.92 (1) Å), whereas the Rh–(μ-CO) distance is slightly larger (cf. Rh_2(μ-CO)(μ-1,3-diene)(η^5-$C_9H_7)_2$,[26] with average Rh–(μ-CO) length of 1.970 (3) Å), again supporting the conclusion of somewhat asymmetric Fe–Rh(μ-CO) bonding in **3b**. Intuitively of course the weaker Rh–(μ-CO) interaction is what is expected due to the presence of the electron-donating DPPE ligand on the Rh atom in **3b**. Indeed the same rational may be used to explain the change in bonding mode of the μ-C_7H_7 moiety on the Fe–Rh framework on going from **1a** to **3b**. In essence, the more electron-rich Rh atom in **3b** requires less electron density from the cycloheptatrienyl ligand than in **1a**, allowing the bridging organic moiety to turn around and coordinate to the Rh atom through the three-carbon allylic fragment only. The Fe–Rh separation at 2.762 (2) Å is much longer than the average value of 2.59 Å found for unsupported Fe–Rh distances;[1a] it is also some 0.116 Å longer than that in the above indenyl complex which contains a bridging CO and bridging 1,3-diene unit. However the metal–metal separation in **3b** is identical with the value found in **1a** (2.764 (1) Å) even though in the present case the metal–metal bonding is supported by a bridging CO unit in addition to the μ-C_7H_7 ring. Clearly the bonding requirements between μ-C_7H_7 and the Fe and Rh atoms appear not to allow for a closer approach of these metals than ca. 2.76 Å.

The other distances and angles within the molecule are normal. As expected the Fe–C(diene) distances are shorter to the inner (average Fe–C = 2.08 (1) Å), than to the outer carbon atoms (average Fe–C = 2.27 (1) Å), although the latter values are longer than commonly observed[27] (range of 2.10–2.18 Å). Similarly the central carbon atom of the allyl unit is marginally closer to the rhodium than to the end carbon atoms, with distances comparing favorably with previous determinations.[28] The Rh–P distances are normal,[29] and as expected the five-membered chelate ring formed by the DPPE ligand is nonplanar.[30] The torsion angles about each bond (Rh–P, 10.9°, 12.7°; P–C, –37.9°, –39.2°; C–C, 49.0°) indicate a symmetrical conformation for the chelating DPPE ligand with carbon atoms on opposite sides of the PRhP plane. Such arrangement appears to be less commonly observed than the unsymmetrical puckering in chelating diphosphine complexes.[30,31] Conformational mobility of the ring is substantial since only one signal is observed for the CH_2 groups in the ^{1}H NMR spectrum of the molecule down to –80 °C.

(24) Green, M.; Jeffery, J. C.; Porter, S. J.; Razay, H.; Stone, F. G. A. *J. Chem. Soc., Dalton Trans.* **1982**, 2475.
(25) Mitschler, A.; Rees, B.; Lehmann, M. S. *J. Am. Chem. Soc.* **1978**, *100*, 3390.
(26) Al-Oboridi, Y. N.; Green, M.; White, N. D.; Bassett, J.-M.; Welch, A. J. *J. Chem. Soc., Chem. Commun.* **1981**, 494.
(27) Cotton, F. A.; Day, V. W.; Franz, B. A.; Hardcastle, K. J.; Troup, J. M. *J. Am. Chem. Soc.* **1973**, *95*, 4522.
(28) (a) Bennett, M. A.; Johnson, R. N.; Robertson, G. B.; Tomkins, I. B.; Whimp, P. O. *J. Organomet. Chem.* **1974**, *77*, C43. (b) McPartlin, M.; Mason, R. *J. Chem. Soc., Chem. Commun.* **1967**, 16.
(29) McAuliffe, C. A.; Levason, W. "Phosphine, Arsine and Stibine Complexes of the Transition Elements"; Elsevier: Amsterdam, 1979.
(30) (a) Hall, M. C.; Kilbourn, B. T.; Taylor, K. A. S. *J. Chem. Soc. A* **1970**, 2539. (b) Pierpont, C. G.; Eisenberg, R. *Inorg. Chem.* **1973**, *12*, 199.
(31) Bonds, W. D., Jr.; Ibers, J. A. *J. Am. Chem. Soc.* **1972**, *94*, 3413.
(32) Band, E.; Muetterties, E. L. *Chem. Rev.* **1978**, *78*, 639 and references therein.

Table VII. $^{13}C\{^1H\}$ NMR Data on Complexes 2 and 3

compd	temp, °C	δ_{Fe-CO}	J_{Rh-C}	δ_{Rh-CO}	J_{P-C} J_{Rh-C}	$\delta_{\mu-CO}$	J_{P-C} J_{Rh-C}	$\delta_{C_7H_7}$	δ_{others} (J_{P-C})	
2a	−30	229.7 (br)		196.9 (dd)	18.8 79.3			62.9 (s)	Me	17.3 (d, 28.5)
2b	−30	227.5 (d)	7.1	201.7 (dd)	18.5 84.5			65.6 (s)	Ph	135.4 (d, 41.3) 133.6 (d, 10.8) 130.4 128.7 (d, 10.8)
3a	−80	230.0 (s)				265.3 (dd)	9.1 21.9	61.7 (s)	Me	17.2 (d, 28.0)
3b	−80	227.1 (s)				261.4 (d)	– 26.7	64.0 (s)	CH_2 Ph	27.8 (t, 22.0) 132.8, 131.8 129.8 (d, 31.0) 128.5
3c	−80	228.2 (s)				258.8 (br)		62.2 (s)	CH_2 Ph	39.7 (t, 8.0) 134.0 131.2 (d, 58.0) 129.8 (d, 45.0) 128.1 (d, 19.0)
3d	−80	229.3 (s)				264.0 (br)		62.0 (s)	CH_2 Me	28.2 (t, 23.0) 17.5 (d, 20.0)

[a] δ relative to Me_4Si, J in Hz, solvent CD_2Cl_2. Abbreviations: s = singlet, d = doublet, t = triplet, br = broad singlet.

The variations in the C–C distances of the μ-C_7H_7 ring are small but nevertheless reflect the bonding interactions between the organic moiety and the metals. The longest distances are associated with C(7)–C(8), 1.44 (1) Å, and C(10)–C(11), 1.47 (1) Å, the bonds linking the diene and allyl fragments of the ring. The distances within the allyl unit are equal (average C–C length is 1.43 (1) Å) and the long–short–long alteration (1.42 (1), 1.39 (2), and 1.43 (2) Å for outer–inner–outer C–C bonds) in the diene group is typical for coordinated diene units.[27] As observed with **1a** and **1b** the bridging cycloheptatrienyl moiety is not planar but adopts the boat conformation; the angle between the normals to the planes formed by the diene and allyl fragment is 53.2°, comparable to the value found in **1a** (56°) but significantly smaller than in **1b** (62°).

Fluxional Behavior and Carbonyl Scrambling in Compounds 2 and 3. The ^1H and ^{13}C NMR data on the complexes **2** and **3** are listed in Tables IV and VII, respectively.

The behavior of the μ-C_7H_7 moiety is predictable. The sharp singlet observed at room temperature remains unchanged at the lowest recorded temperatures indicating rapid ring whizzing of the cycloheptatrienyl ring similar to that observed in **1a** and **1b**.

The molecules also undergo interesting carbonyl scrambling processes which merit close scrutiny. Since IR spectroscopy showed that compounds **3** exist in solution exclusively in the carbonyl-bridged form D found in the solid state, the behavior of these molecules is discussed first. Figure 4 shows the variable-temperature ^{13}C NMR spectra of **3b** in the carbonyl region. The low-temperature limiting spectrum consists of two signals in a 1:2 ratio in the regions normally associated with bridging and terminal CO ligands respectively. The former signal is split into a doublet due to ^{103}Rh–^{13}CO coupling; coupling to ^{31}P is not observed. Reference to Table VII shows that the other compounds **3** have similar features in their ^{13}C NMR spectra at low temperature indicating carbonyl-bridged structure for these molecules as well. As the temperature of NMR probe is raised the carbonyl signals broaden, coalesce, and merge into a sharp singlet by +40 °C, indicating rapid bridge–terminal carbonyl group exchange. Application of the approximate expression for coalescence of nonequal singlets[33] yields $\Delta G^{\ddagger}_{253}$ of 10.3 kcal/mol for the exchange process in **3b**. There are essentially two types

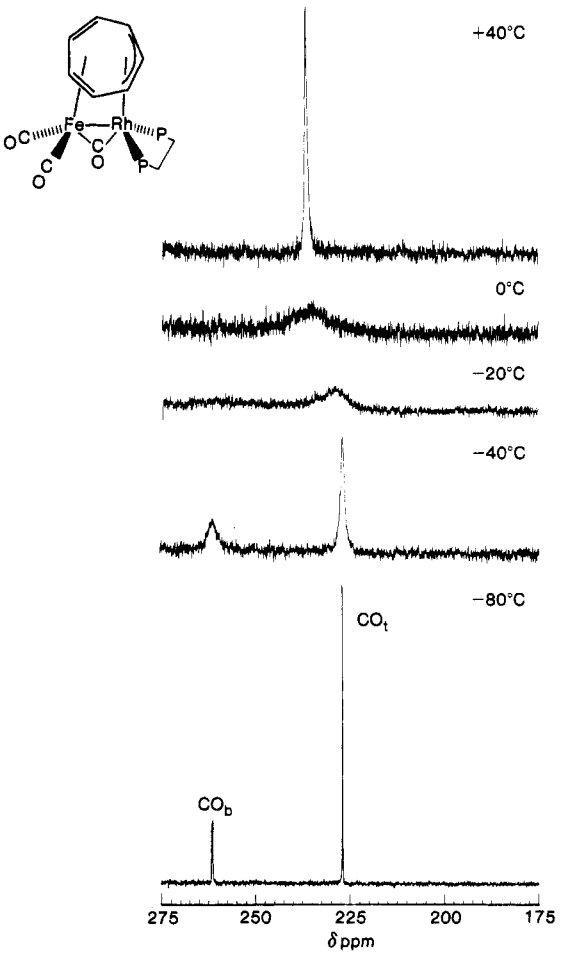

Figure 4. Variable-temperature ^{13}C NMR spectra of **3b** in the carbonyl region.

Scheme II. Bridge-Terminal Carbonyl Group Exchange in 3b

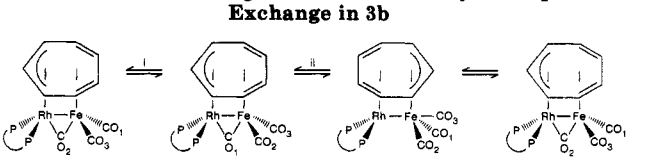

of mechanisms that have been identified to account for bridge–terminal carbonyl group exchanges in binuclear systems: (a) concerted, two for two bridge opening and

(33) Shanon-Atidi, H.; Ban-Eli, K. H. *J. Phys. Chem.* **1970**, *74*, 961.

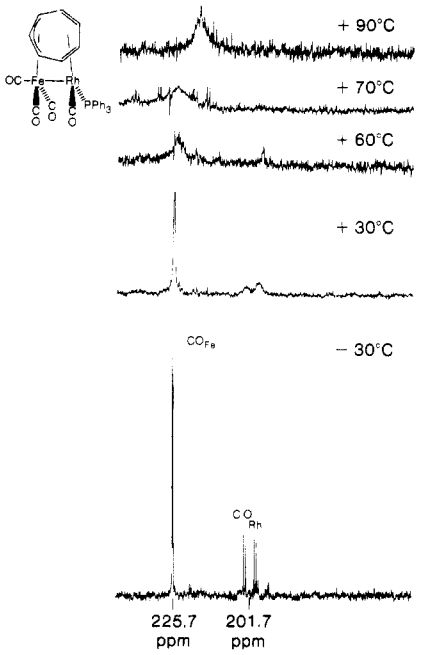

Figure 5. Variable-temperature ^{13}C NMR spectra of **2b** in the carbonyl region.

closing and (b) one for one bridge opening and closing. The former process that would put one of the phosphorus atoms of the DPPE ligand into the bridging position is clearly unavailable in the present context. As illustrated in Scheme II, mechanism b can be subdivided into (i) a synchronous one for one bridge–terminal exchange and (ii) a stepwise process via an unbridged intermediate. Although mechanistic delineation between the two remain elusive, the ready accessibility of the unbridged form, due to the variable bonding capability of the μ-C_7H_7 ligand, makes us favor path ii for the carbonyl scrambling in **3b** and in related compounds. This is in interesting contrast to $Cp_2Rh_2(\mu\text{-}CO)(CO)L$ (L = $P(OPh)_3$, PMe_2Ph, CO) where, presumably due to the electronic imbalance that an unbridged intermediate would produce, the synchronous process for carbonyl exchange was favored.[34,35] Before concluding the discussion on compounds **3**, it is worth emphasizing that although carbonyl group exchange may be related to bonding mode change of the μ-C_7H_7 moiety, ring whizzing of the latter group is not intimately coupled to carbonyl scrambling in the molecules. Indeed, ring whizzing is a much lower activation energy process as evidenced by the temperature invariant nature of the sharp, averaged singlet associated with the bridging cycloheptatrienyl moiety.

The variable-temperature ^{13}C NMR spectra of **2b** in the carbonyl region is shown in Figure 5. At low temperatures the spectrum consists of two signals which remained unchanged down to −90 °C. The resonance at 201.7 ppm can be assigned unequivocally to a terminal carbonyl group on rhodium atom split by both ^{103}Rh and ^{31}P nuclei. The doublet at 225.7 ppm is in a region typical of terminal CO groups on iron; the coupling is due to ^{103}Rh as verified by heteronuclear decoupling of ^{31}P which left the doublet feature intact. Warming the sample caused broadening

Scheme III. Localized and Global Carbonyl Group Exchange in 2b

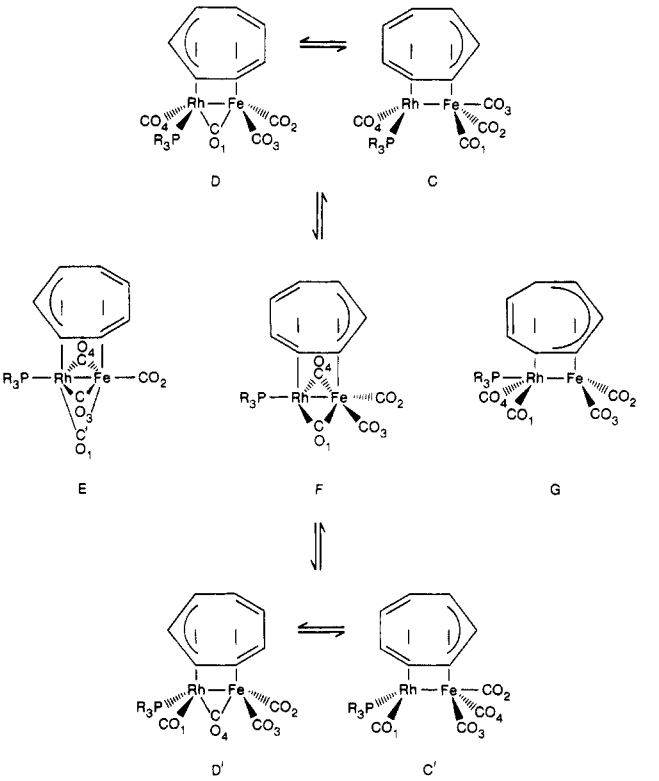

of the resonances, coalescence, and the appearance of a single broad line at +90 °C. Although the line-shape changes were reversible with temperature, significant decomposition of the compound at higher temperatures resulted in poor spectral qualities and prevented the recording of the fast-exchange spectrum.

The simple spectrum at low temperature is clearly inconsistent with either structure C or D and even less so with a mixture of the two as indicated by the IR spectrum of the compound, unless there is rapid carbonyl scrambling. Although the low-temperature process is quite specific and involves only the carbonyls on iron, it can be achieved simply by rapid equilibrium between the all-terminal, C, and bridged, D, isomers of **2b**. Indeed, reference to the top part of Scheme III reveals that this process will only cause movement of a terminal CO group of iron into bridging position and back again to a terminal position on the same iron atom as long as the favored η^4,η^3-bonding mode of the bridging cycloheptatrienyl unit is maintained. Thus, once again one for one bridge-forming and -opening process, assisted by the μ-C_7H_7 functionality, appears to be responsible for the rapid scrambling of CO groups on iron. The alternate explanation that low temperatures favor the all terminal form C, which undergoes carbonyl scrambling on iron, as already observed for **1a**,[2] is less favored because of the coupling between ^{103}Rh and the $Fe(CO)_3$ fragment. In the parent molecule **1a**, which is known to exist exclusively as the all terminal isomer, the signal due to $Fe(CO)_3$ is a sharp singlet and the same would be anticipated for an all terminal **2b**. On the other hand, the observed coupling is clearly consistent with the intervention of the bridging form. As expected from the presence of both isomers in solution the localized carbonyl scrambling on iron is more rapid in the monophosphine-substituted molecules **2** than in the strictly CO-bridged, disubstituted compounds **3**.

At higher temperatures the appearance of a single averaged carbonyl signal heralds the onset of intermetallic

(34) (a) Evans, J.; Johnson, B. F. G.; Lewis, J.; Matheson, T. W.; Norton, J. R. *J. Chem. Soc., Dalton Trans.* **1978**, 626. (b) Evans, J.; Johnson, B. F. G.; Lewis, J.; Matheson, T. W. *J. Chem. Soc., Chem. Commun.* **1975**, 576.

(35) Synchronous exchange of bridging and terminal carbonyl groups appears to operate in $(L\text{–}L)Fe_2(CO)_7$ type molecules as well: Cotton, F. A.; Haines, R. J.; Hanson, B. E.; Sekutowski, J. C. *Inorg. Chem.* **1978**, *17*, 2010 and references therein.

exchange of carbonyl groups. As shown in Scheme III there are several plausible intermediates which would allow for carbonyl group migration between Fe and Rh. We favor the doubly bridged structure F since it is easily achieved from both isomeric C and D and it maintains the favored μ-η^4,η^3-C_7H_7 bonding functionality. Furthermore, the process is related to the well-established merry-go-round mechanism for carbonyl group migration in di- and polynuclear metal carbonyl compounds.[32] An often observed feature in these systems is increased facility for carbonyl group migration upon phosphine substitution.[32,36] This is well illustrated in the present context as well. The parent pentacarbonyl **1a** shows no line broadening in the ^{13}C NMR spectrum up to 70 °C whereas in **1b** this temperature represents the coalescence point with an associated ΔG^*_{343} of 15.4 kcal/mol.

Conclusion

It is apparent from this first reactivity study on **1a** that the bridging cycloheptatrienyl moiety is capable of exhibiting a variety of bonding capabilities. This flexible nature can be manifested in two distinct manners. The ability to create coordinative unsaturation is responsible for the facile carbonyl substitution reaction and may promote other reactions as well. The capacity for bonding mode changes between the Fe–Rh framework and the μ-C_7H_7 ligand is the reason for the movement of terminal CO group to bridging position and the associated CO scrambling processes.

Further studies are underway to delineate the scope of the reactivity of **1a**. The synthesis of related (μ-C_7H_7)-$MM'(CO)_5$ (M = Fe, Ru, Os and M' = Co, Rh, Ir) compounds are also being explored in order to probe the effect of the metal on the structure, fluxionality, and reactivity in this class of molecules.

Acknowledgment. We thank the Natural Sciences and Engineering Research Council of Canada and the University of Alberta for financial support of this work and Johnson Matthey for generous loan of rhodium trichloride. F.E. acknowledges a Feodor Lynen research fellowship from the Alexander von Humboldt Foundation, Bonn, West Germany.

Registry No. **1a**, 51608-48-1; **1b**, 100190-09-8; **2a**, 91868-00-7; **2b**, 91855-30-0; **3a**, 91855-31-1; **3b**, 91855-32-2; **3c**, 91855-33-3; **3d**, 91855-34-4; **3e**, 100190-10-1; **3f**, 100190-11-2; $Na(C_7H_7)Fe(CO)_3$, 62313-81-9; $[RhCl(COD)]_2$, 12092-47-6; Rh, 7440-16-6; Fe, 7439-89-6.

Supplementary Material Available: A table of thermal parameters for **1b** (Table VIII) and listings of observed and calculated structure amplitudes for **1b** and **3b** (31 pages). Ordering information is given on any current masthead page.

(36) Mersalla, J. A.; Caulton, K. G. *Organometallics* **1982**, *1*, 274.

Synthesis, Molecular Structure, Solution Dynamics, and Reactivity of (η-C_5H_5)$_2$M(μ-PR_2)$_2$Rh(η-indenyl) (M = Zr, Hf; R = Et, Ph)†

R. T. Baker* and T. H. Tulip

Central Research & Development Department, E. I. du Pont de Nemours & Company, Experimental Station, Wilmington, Delaware 19898

Received June 13, 1985

The "metal-containing diphosphines", $Cp_2M(PR_2)_2$ (Cp = η-C_5H_5; M = Zr, Hf; R = Et, Ph), displace both coordinated ethylenes from (η-C_2H_4)$_2$Rh(η-indenyl), yielding the early–late heterobimetallic complexes $Cp_2M(\mu$-$PR_2)_2Rh(\eta$-indenyl). The molecular structure of $Cp_2Zr(\mu$-$PPh_2)_2Rh(\eta$-indenyl) (**1c**), determined by X-ray diffraction, consists of edge-shared, pseudotetrahedral 16e Zr(IV) and distorted, square-planar Rh(I) centers with a planar ZrP_2Rh bridging unit and a Zr···Rh separation of 3.088 (1) Å. The indenyl ligand exhibits a pronounced "slip-fold" distortion toward η^3-coordination and high barriers (14–15 kcal/mol) to indenyl rotation are observed by ^1H DNMR. Addition of CH_3I to $Cp_2M(\mu$-$PEt_2)_2Rh(\eta$-indenyl) affords the cationic d^0–d^6 heterobimetallics $[Cp_2M(\mu$-$PEt_2)_2Rh(CH_3)(\eta$-indenyl)]I. Red crystals of **1c** are monoclinic, $P2_1/m$ (no. 11), with two molecules per unit cell of dimensions a = 9.700 (1) Å, b = 18.855 (3) Å, c = 10.185 (1) Å, and β = 112.95 (1)°. The structure was refined to R = 0.029 and R_w = 0.031 for 2928 observed reflections.

Transition-metal complexes containing the η-indenyl ligand undergo ligand substitution much more readily than their η-cyclopentadienyl analogs due to the stability of the η^3 bonding mode in the former, suggested to result from the aromatization of the indenyl benzene ring.[1] The recently reported[2,3] "metal-containing diphosphines", $Cp_2M(PR_2)_2$ (Cp = η-C_5H_5; M = Zr, Hf; R = Et, Ph, cyclohexyl (Cy)), contain both 1e and 3e donor PR_2 ligands. Donation of both phosphorus lone pairs to a second metal center thus creates an electronically unsaturated early metal center in the resulting PR_2-bridged heterobimetallic complex. We have previously described the binding of various metal carbonyl[4] and ML_n[5] fragments, where M = Ni, Pd,

† Contribution no. 3775.

(1) (a) Hart-Davis, A. J.; Mawby, R. J. *J. Chem. Soc. A* **1969**, 2403. (b) White, C.; Mawby, R. J.; Hart-Davis, A. J. *Inorg. Chim. Acta* **1970**, *4*, 441. (c) Jones, D. J.; Mawby, R. J. *Ibid.* **1972**, *6*, 157. (d) Eshtiagh-Hosseini, H.; Nixon, J. F. *J. Less Common Met.* **1978**, *61*, 107. (e) Caddy, P.; Green, M.; O'Brien, E.; Smart, L. E.; Woodward, P. *Angew. Chem., Int. Ed. Engl.* **1977**, *16*, 648; *J. Chem. Soc., Dalton Trans.* **1980**, 962. (f) Caddy, P.; Green, M.; Howard, J. A. K.; Squire, J. M.; White, N. J. *Ibid.* **1981**, 400. (g) Bottrill, M.; Green, M. *Ibid.* **1977**, 2365. (h) Gal, A. W.; van der Heijden, H. *Angew. Chem., Int. Ed. Engl.* **1981**, *20*, 978. (i) Diversi, P.; Giusti, A.; Ingrosso, G.; Lucherini, A. *J. Organomet. Chem.* **1981**, *205*, 239. (j) Rerek, M. E.; Ji, L.-N.; Basolo, F. *J. Chem. Soc., Chem. Commun.* **1983**, 1208. (k) Rerek, M. E.; Basolo, F. *J. Am. Chem. Soc.* **1984**, *106*, 5908. (l) Casey, C. P.; O'Connor, J. M. *Organometallics* **1985**, *4*, 384.

0276-7333/86/2305-0839$01.50/0